Published in final edited form as:

Anal Biochem. 2013 April 15; 435(2): 140–149. doi:10.1016/j.ab.2012.12.021.

A Sandwich ELISA for Measuring Benzo[*a*]pyrene-albumin Adducts in Human Plasma

Ming Kei Chung[a], **Luca Giovanni Regazzoni**[a], **Michael McClean**[b], **Robert Herrick**[c], and **Stephen M. Rappaport**[a,*]

[a]Center for Exposure Biology, School of Public Health, University of California, Berkeley, CA, USA

[b]Department of Environmental Health, Boston University School of Public Health, Boston, MA, USA

[c]Exposure, Epidemiology and Risk Program, Department of Environmental Health, Harvard School of Public Health, Boston, MA

Abstract

Exposures to polycyclic aromatic hydrocarbons (PAHs) have often been quantified via DNA or human-serum albumin (HSA) adducts of the carcinogenic metabolite, benzo[*a*]pyrene diolepoxide (BPDE). We previously reported a sandwich ELISA, using 8E11 as capture antibody and anti-HSA as detection antibody, that detected intact BPDE adducts in HSA isolated from plasma. After confirming that BPDE binds to HSA at His146 and Lys195, we modified the ELISA to measure intact BPDE-HSA directly in human plasma. To adjust for interferences due to nonspecifically bound HSA on well surfaces and to cross reactivity of the antibodies, the ELISA employs paired wells with and without addition of BPDE tetrols to deactivate 8E11. By performing assays in quadruplicate, a series of sample-specific adjustments and screening steps are used to reduce measurement errors that are a consequence of detecting low BPDE-HSA concentrations in the general population. ELISA measurements of BPDE-HSA in plasma from smoking and nonsmoking subjects (range: 0.335 – 0.941 ng BPDE-HSA/mg HSA; 4.59 – 47.2 fmol BPDE-HSA/mg HSA) and from highway workers with and without exposures to asphalt emissions (range: 0.346 – 13.8 ng BPDE-HSA/mg HSA; 5.68 – 228 fmol BPDE-HSA/mg HSA) detected differences in BPDE-HSA levels in the *a priori*- expected directions.

Keywords

ELISA; biomonitoring; PAHs; benzo[*a*]pyrene; human serum albumin; background adjustment

[*]**Corresponding author:** Stephen M. Rappaport, Professor of Environmental Health, School of Public Health, University of California, Berkeley, CA 94720-7356, USA, Tel: +1 510 642-4355, Fax: +1 510 642-5815. srappaport@berkeley.edu.

Financial Support

Financial support for this work was provided by a contract from the Long-range Research Initiative of the American Chemistry Council and by grant U54ES016115 from the U.S. National Institute of Environmental Health Sciences (NIEHS) through the trans-NIH Genes, Environment, and Health Initiative.

Introduction

Polycyclic aromatic hydrocarbons (PAHs) are ubiquitous pollutants produced by incomplete combustion of hydrocarbons and are constituents of cigarette smoke, engine exhausts, industrial effluents and grilled and smoked foods [1; 2]. The class of PAHs contains several hundred compounds with two or more fused aromatic rings. Exposures to PAHs cause human cancers, particularly of the lung, bladder and skin [3; 4; 5]. Prenatal exposures to PAHs have been associated with low birth weight, premature delivery and a host of developmental problems in children [6; 7; 8; 9].

Given the structural diversity of PAHs, the assessment of exposures to these toxic species has been challenging. Studies measuring dozens of PAHs in air, soil, water and dust [10; 11; 12; 13] have been useful for apportioning sources of PAHs in environmental samples [14]. However, because humans are simultaneously exposed to PAHs from air, water and food, measurement of all sources is impractical for investigations of PAH-related health effects. This diversity of exposure sources has motivated biomonitoring as an alternative to environmental monitoring for evaluating PAH exposures. Once absorbed in the body, PAHs are metabolized by cytochrome P450 enzymes to reactive molecules that either bind with macromolecules such as DNA and proteins to form adducts [15; 16] or are hydrolyzed and excreted in urine and feces.

Applications of PAH-DNA adducts as biomarkers of exposure and early toxicity have been reported since the 1980s [17]. Indeed, because PAH-DNA adducts can be detected with the ultra sensitive ^{32}P-postlabeling assay (1 adduct per 10^{10} nucleotides), these adducts have been among the most popular biomarkers ever used by molecular epidemiologists [18]. However, such applications of PAH-DNA adducts have inherent disadvantages. First, the only practical source of DNA in human biospecimens is peripheral blood mononuclear cells, which include cell types having a hundred-fold range of life spans [19] and differential rates of DNA repair and adduct stability [20]. Second, the ^{32}P-postlabeling assay is laborious and includes several steps that introduce significant variability [18; 21; 22], leading to inter-laboratory coefficients of variation (CV) as high as 108% [22; 23; 24]. Third, the postlabeling assay detects all stable and bulky DNA modifications *en masse* and is, therefore, not specific for PAH generally or for quantifying particular PAHs of interest [25].

To simplify exposure assessment in epidemiologic research and health surveillance, benzo[*a*]pyrene (BaP) - a 5-ring PAH and potent carcinogen - has been used as a surrogate marker for PAHs in environmental samples. Mammalian metabolism converts BaP to the reactive benzo[*a*]pyrene diol epoxide (BPDE), which forms adducts with DNA and proteins [17] and is hydrolyzed to BPDE tetrols that are excreted. Although formation of DNA adducts (BPDE-DNA) has direct relevance to cancer development [26], the low abundance of DNA in blood plus the high turnover rate of DNA adducts [27] makes BPDE-DNA a less-than-optimal surrogate for BaP exposure. As an alternative to BPDE-DNA, adducts of BPDE with human serum albumin (HSA) (BPDE-HSA) have been used for human biomonitoring [28; 29; 30; 31]. The concentration of HSA is more than a thousand-fold greater than that of DNA in human blood (45 mg HSA/ml vs. 28 μg DNA/ml) and, unlike DNA adducts, HSA adducts are not repaired. Thus BPDE-HSA should be a relatively stable

biomarker of BaP exposure, with an estimated human half-life of 20 days that ensures integration of BaP exposures over about a month [32].

Several assays, including high-performance liquid chromatography (HPLC) with detection by fluorescence or mass spectrometry (MS) and competitive enzyme-linked immunosorbent assays (ELISA) have been used to measure BPDE-HSA in heavily modified samples [32]. However, to permit detection of BPDE-HSA in humans exposed to PAHs in occupational and environmental settings, these adducts are usually hydrolyzed to BPDE tetrols that are then enriched prior to analysis [31; 32; 33; 34]. This is problematic because consistent and reliable quantitation of the BPDE tetrols depends on the particular hydrolysis conditions [33; 34] that vary across studies [32; 35]. In our view, this need to precisely convert BPDE to tetrols hinders use of BPDE-HSA as a biomarker of PAH exposure in epidemiological studies.

We previously developed a sandwich ELISA for BPDE-HSA, using 8E11 as capture antibody and anti-HSA as detection antibody, that readily detected intact BPDE adducts in HSA isolated from plasma of steel-factory workers exposed to moderate and high levels of PAHs [36]. Although the detection system was able to measure intact BPDE-HSA directly in plasma or serum, we could not routinely apply the ELISA to plasma from populations exposed to low PAH levels due to high and varying background readings. We subsequently traced the background signal to amplification of the anti-HSA detection antibody in response to unadducted HSA that was non-specifically bound to well surfaces and to possible cross reactivity of anti-HSA with interfering molecules.

Here we describe enhancements to the sandwich assay for measuring intact BPDE-HSA adducts directly in plasma from subjects exposed to PAH at low levels. As shown in Figure 1, the major innovation involves parallel measurements of BPDE-HSA and BPDE-tetrol-deactivated 8E11 to adjust for background readings. These parallel measurements employ a sample-specific calibration procedure to remove bias as well as a sample-screening step to minimize measurement errors. We validated the assay with plasma samples from smokers and nonsmokers and from a group of highway workers exposed to PAHs from use of asphalt. Finally, because our previous work suggested that BPDE reacted with HSA at two loci, we performed proteomics to confirm the modification sites as His146 and Lys195.

Materials & Methods

Human plasma samples

Archived plasma was obtained from two previous studies that had been conducted under human-subject protocols approved by institutional review boards at the University of North Carolina [37] and Harvard University [38; 39] between 1998 and 2000. The first sample was obtained from a group of 191 young healthy adult volunteers that had been recruited to investigate the variability of benzoquinone-HSA adducts in the general population [37]. Since subjects had been equally divided between smokers and nonsmokers, our interest here was to determine whether levels of BPDE-HSA were associated with self-reported smoking status and intensity. Immediately after blood collection, red blood cells were removed by centrifugation and washed with an equal volume of phosphate-buffered saline (PBS), which

was combined with the plasma. Samples of diluted plasma were stored at −80°C for 13 y prior to the current investigation. After thawing, specimens were pooled to ensure the anonymity of subjects by combining aliquots of plasma from 4 or 5 subjects based on race (black or white), gender and self-reported smoking status; there were 35 pooled samples from 158 subjects. Aliquoted samples were stored at −80°C for approximately three months prior to ELISA analysis and underwent two freeze-thaw cycles. Smoking intensity was quantified as the average number of cigarettes smoked per day for subjects in each pooled sample.

A second set of 80 plasma samples was selected from 203 specimens derived from 85 highway-paving and construction workers [38; 39]. The 80 plasma samples analyzed in the current investigation were obtained from 28 highway-paving workers who used asphalt (paver operators, screedmen and rakers) and 9 highway-construction workers who did not use asphalt. All of these workers were either white or Hispanic nonsmokers. Because the longitudinal study involved repeated blood collection, the 37 workers in the current sample had either 2 or 3 plasma samples (median = 2) collected during different seasons of the year. A Ficoll centrifugation procedure had been used to separate red blood cells, plasma and mononuclear white blood cells. Plasma was aliquoted and stored at −20°C for 6 y and at −80°C for an additional 6 y prior to the current investigation (one freeze-thaw cycle).

All plasma samples were assigned random numbers and the analyst was blinded as to exposure status and other characteristics of samples.

A fresh sample of human plasma was obtained by venipuncture from a laboratory volunteer for preparation of plasma containing known amounts of BPDE-HSA for determination of accuracy and precision. Ten ml of blood were kept at 4°C for 30 min and then centrifuged at 200 g for 10 min to remove red blood cells. Plasma was aliquoted into 1-ml portions and stored at −80°C prior to addition of known amounts of BPDE-HSA.

Chemicals and reagents

The following chemicals and reagents were obtained from the indicated vendors: Fisher Scientific (Pittsburgh, PA): ThermalSeal® adhesive films, tris-buffered saline (TBS, 10x), acetic acid (glacial, ACS grade), sulfuric acid (ACS grade), dimethyl sulfoxide (DMSO), methanol (LCMS grade), TCEP, acetic acid (LCMS grade), formic acid (Optima®, LCMS Grade), acetonitrile (Optima grade, 99.9%); Sigma-Aldrich: carbonate-bicarbonate buffer, Tween 20, HSA (lyophilized powder, 97–99%), porcine trypsin, ammonium bicarbonate, sodium azide; Bethyl Lab, Inc.: goat anti-human albumin IgG, biotinylated; Thermo Scientific (Rockford, IL): SuperBlock®, ultra-sensitive ABC Peroxidase kits, one-step ultra TMB, goat anti-mouse IgG, Fc fragment specific (ImmunoPure®, min. cross-reactivity); Bethyl Laboratories, Inc. (Montgomery, TX): goat anti-human-albumin IgG, HRP conjugated (A80–129P); goat anti-human albumin IgG (A80–129A), TMB peroxidase substrate; Santa Cruz Biotech, Inc. (Santa Cruz, CA): 8E11; MRI Global (Kansas City, MO): tetrols powder (Benzo[*a*]pyrene-r-7, t-8, t-9, c-10-tetrahydrotetrol(+/−), MRI # 472); Genesee Scientific (San Diego, CA): nonfat dry milk (NFDM).

Determination of HSA-modification sites

A shotgun-proteomic approach was used to identify the BPDE modification sites on HSA. A BPDE-HSA standard was prepared as previously described (39) starting with a 2 mg/ml HSA solution incubated with 30 μM BPDE (HSA:BPDE 1:1 molar ratio). A 50 μL aliquot containing 100 μg of BPDE-HSA was diluted 1:1 with 20% methanol in 100 mM ammonium bicarbonate. After adding TCEP to 5 mM, the solution was incubated at 37 °C for 15 min in the dark to reduce disulfide bonds. Then trypsin was added at a 1:10 (w:w) protease:protein ratio and digestion was performed at 37 °C with a pressurized system (Barocycler NEP2320, Pressure Biosciences Inc., South Easton, MA) that was programmed to generate 30 pressure cycles between ambient (15 s) and 1380 bar (45 s).

After diluting the tryptic digest 1:10 with water/acetonitrile/formic acid (94.9/5/0.1; v/v/v) in a clear glass HPLC vial (National Scientific, Rockwood, TN) the digest was stored at −80 °C prior to proteomics analysis. A 40-μl aliquot was injected into an HPLC (series 1200, Agilent, Santa Clara, CA, USA) coupled to a high-resolution MS (LTQ Orbitrap XL hybrid mass spectrometer with an Ion Max electrospray ionization (ESI) source (Thermo Fisher Scientific, Waltham, MA). Chromatographic separation was accomplished with a Zorbax 300SB C8 column (1.0×150 mm, 3.5-μm particle size) (Agilent, Santa Clara, CA) at a flow rate of 80 μl/min. The sample was loaded onto the column and cleared of the matrix with 98% buffer A (0.1% formic acid in water) and 2% buffer B (0.1% formic acid in acetonitrile) for 5 min and then programmed to 60% B over 60 minutes. After elution of peptides, the system was ramped to 95% B over 5 minutes to wash the column and then returned to initial conditions for 25 minutes.

The ESI source was operated at a spray voltage of 2.8 kV, a nebulizer gas (nitrogen) flow rate set at 15 (a.u.), a capillary temperature of 250° C and a capillary voltage of 20 V. The column and sample compartments were maintained at 35 and 4°C, respectively. The MS performed scan cycles in data-dependent mode and acquired mass spectra using the Orbitrap with the following settings: positive-ion profile mode, full scan range 250–1,500 m/z, AGC target 5×10^5, 500 ms maximum inject time, microscan set to 1, resolving power 60,000 (FWHM at *m/z* 400). For each MS scan the three most intense ions exceeding a count of 2×10^4 were selected for MS/MS analysis in the linear ion trap using both CID and ETD activation with the following settings: centroid mode, precursor ions isolation width of 3 m/z, AGC target 1×10^4, 100 ms maximum inject time, microscan set to 1. A normalized collision energy of 28 and an activation time of 30 ms were used for collision induced dissociation (CID). Electron transfer dissociation (ETD) was triggered by the fluoranthene anion using an activation time of 200 ms. Dynamic exclusion was enabled to reduce redundant MS/MS spectra acquisition as follows: 2 repeat counts, 30 s repeat duration, exclusion list size 500, 90 s of exclusion duration, relative exclusion mass ± 20 ppm. Charge state screening and monoisotopic precursor selection were enabled, singly and unassigned charged ions were not fragmented. A list of 7 background compounds reported by Keller *et al.* [40] were used as lock masses to provide a real time internal mass calibration during the analysis. Instrument control was provided by Xcalibur software (2.07, Thermo Fisher Scientific).

MassMatrix was used as the primary search engine for the identification of BPDE modification sites on HSA. According to the proposed mechanism by Day *et al.* [29], 302.094294 Da was as the monoisotopic mass for BPDE modifications at Arg, His, Lys, Cys, Asp and Glu residues. UniProt entry P02768 was selected as the HSA sequence for mapping. We selected 'Trypsin, no P rule' for the *in silico* digestion and allowed for 2 maximum missed cleavages. Peptide and fragment ions tolerance were set to 10 ppm and 0.8 Da respectively. Other parameters were used as in the default profile for protein identification. Similar settings were also applied to the OMSSA Browser (v.2.1.1, National Library of Medicine), which was used as a secondary search engine to reduce false positive identification. All the precursor ion masses and the associated fragmentation patterns of the identified modifications from search engines were reviewed and cross-checked manually using the peptide sequence fragmentation modeling function available in Molecular Weight Calculator (v.6.49, Pacific Northwest National Laboratory, US Department of Energy).

Sandwich ELISA for BPDE-HSA

As shown in Figure 1, the basic sandwich ELISA procedure has the same components as the original version [36], namely, a spacer consisting of anti-mouse Fc antibody, 8E11 as capture antibody, biotinylated anti-HSA as detection antibody and an ABC amplification system. However, particular antibodies and reagents were changed to reduce background effects and to increase sensitivity. For example, use of an ultra-sensitive ABC staining kit increased sensitivity about 5-fold. The major change to the assay involves parallel ELISA measurements with and without BPDE tetrol-deactivated 8E11 to adjust for background effects due to non-specific binding of HSA and potential cross reactivity of anti-HSA.

After thawing, 400 μl of plasma was centrifuged at 13,000 g for 10 min to remove potential interfering species. An aliquot of 335 μl was carefully withdrawn from the upper half of the plasma and made up to 15% NFDM and 0.02% sodium azide. Since readings are required with and without addition of BPDE tetrols, plasma was split into two portions at 30 μl/well, one diluted with a 3,000 ppm BPDE tetrol solution to a tetrol concentration of 60 ppm ('background' well in Figure 1) and the other diluted to an equivalent concentration of DMSO (0.034%) ('sample' well in Figure 1). All plasma samples were measured in quadruplicate (4 pairs of wells, Figure 1).

Unless otherwise mentioned, plates were incubated at 37°C for 45 min and - between loading steps to minimize non-specific binding of HSA - were rinsed 3 times with TBS-T (0.1% Tween) at 200 μl/well prior to incubation and 5 times after incubation. All reagents and samples were dissolved in 15% NFDM. In brief, goat anti-mouse IgG (Fc specific) was coated in the wells of a 96 well plate (MaxiSorp™, C type, Nunc, NY) at 10 μl/ml (in 0.1M carbonate-bicarbonate buffer, 30 μl/well) and incubated overnight at 4°C, followed by blocking with 15% NFDM (250 μl/well) and loading of 8E11 at 3.34 μg/ml (20 μl/well). Then, samples and standards were transferred to the plate at 30 μl/well in quadruplicate with 4 pairs of wells containing 8E11 and BPDE tetrol-deactivated 8E11, respectively. The detection antibody, biotinylated goat anti-HSA IgG prepared in SuperBlock®, was added at 1 μg/ml, 20 μl/well before the addition of ultra ABC (20 μl/well) and the mixture was allowed to stand for 30 min at room temperature. Then, ultra TMB was added (20 μl/well)

and incubated for 30 min at room temperature in the dark. Finally, the reaction was stopped by adding 20 μl of a mixture of 8.5 M acetic acid and 0.5 M sulfuric acid. Color intensity was measured at 450 nm with a microplate spectrophotometer (ELx800, Bio-Tek, Winooski, VT).

ELISA measurement of HSA

The HSA concentrations of plasma samples were measured by a sandwich ELISA with a dynamic range of 1 to 200 ng/ml. Plasma samples were assayed (in duplicate) at 3 consecutive 4-fold dilutions. Unless otherwise specified, plates were rinsed 3 times between incubations with 200 μl/well of TBS-T (0.05% Tween); all reagents, samples and antibodies were loaded at 50 μl/well with 5% NFDM; and plates were incubated at 37^{O}C for 45 min for each step. Goat anti-human-albumin IgG (0.5 μg/ml in 0.1 M carbonate-bicarbonate buffer) was coated on a 96-well plate (MaxiSorp™, C type, Nunc, NY) at 4°C overnight. After blocking with 5% NFDM at 200 μl/well, diluted samples that should fall in into the range covered by the standard curve (3.1 to 200 ng/ml) were loaded. Then, goat anti-human-albumin IgG, conjugated HRP (0.2 μg/ml in 5% NFDM) was added and plates were incubated. Finally, TMB solution was loaded and plates were incubated for 25 min in the dark at room temperature. Color intensity was measured at 630 nm with a microplate spectrophotometer (ELx800, Bio-Tek, Winooski, VT). A calibration curve was fitted to a 4-parameter logistic function with Masterplex ReaderFit (v 2.0.0.76, Hitachi Solutions America, Ltd, San Francisco, CA).

Calibration of BPDE-HSA

A BPDE-HSA standard was prepared at 2 mg/ml as described [36] but using a 1:1 BPDE-to-HSA ratio. Since calibration requires readings with and without BPDE tetrol-deactivated 8E11, standard solutions were split into two portions at 30 μl/well, one diluted with a solution of 3,000 ppm BPDE-tetrol in DMSO to a tetrol concentration of 60 ppm and the other diluted to an equivalent concentration of DMSO (0.034%). Standards were measured using the sandwich assay for BPDE-HSA described above at concentrations of 0.156, 0.313, 0.625, 1.25, 2.5, 5, 10, 20 ng BPDE-HSA/well.

Since the traditional calibration method for ELISA overestimates BPDE-HSA levels measured from our design (mainly from the nonspecific binding of HSA to well surfaces) we individually adjusted each BPDE-HSA concentration for the background reading in that plasma sample. As described above, pairs of ELISA readings were obtained for BPDE-HSA standards and a standard curve was constructed from the absorbance difference in each pair. Calibration involved fitting the BPDE-HSA standard curve with Qtiplot (v. 0.9.8.3, ProIndep Serv SRL) using the following sigmoid function:

$$y = min + \frac{max - min}{1 + 10^{[\log(IC50) - x]Hillslope}} \quad (1)$$

where min and y are the minimum absorbance and total absorbance for a given standard pair, respectively, max is the maximum absorbance plateau from the calibration curve, log(IC50)

is the log (base 10) of *IC*50 from the calibration curve, *x* is the log (base 10) concentration of BPDE–HSA (ng/mg HSA), and *Hillslope* is the slope factor from the calibration curve. As shown in Figure 2, a family of calibration curves is produced to adjust for background readings across plasma samples analyzed with a given set of standards. Quantitation involves substituting the absorbance readings from the background and sample wells of a given sample for *min* and *y*, respectively, in Eq. (1) and then solving for 10^x, which represents the BDE-HSA concentration. Calculations were performed with an Excel spreadsheet (v. 14, Microsoft Office 2010).

Screening samples for valid measurements

We observed that some plasma samples contained interfering substances that led to invalid detection of BPDE-HSA [i.e. $min > y$, which is uninterpretable via Eq. (1)] and, occasionally, to great intra-sample variability caused by an anomalously high reading in a replicate. To reduce potential errors from such interferences, a pair of screening rules was used to screen for invalid readings. A sample was designated as invalid if 3 of the 4 paired measurements had $min > y$ absorbance readings or if BPDE-HSA levels differed by more than 10-fold across quadruplicate measurements. Invalid samples were re-assayed and the same criteria were applied. If the second determination was also invalid, then the sample was treated as a missing observation in statistical analyses.

Detection limit and assay precision

The detection limit (DL), defined as 3 times the background signal, was estimated at 0.2 ng BPDE-HSA/mg HSA (3.28 fmol BPDE equivalents/mg HSA). The precision and accuracy of the sandwich ELISA were assessed with samples of plasma containing known quantities of BPDE-HSA. A 1-ml aliquot of frozen plasma from a volunteer subject was thawed and 400 μl was centrifuged at 13,000 g for 10 min. An aliquot of 335 μl was carefully withdrawn from the upper half of the plasma and made up to 15% NFDM and 0.02% sodium azide. This plasma sample was spiked with BPDE-HSA at 10 ng/30 μl, aliquoted and stored at −80 °C prior to use. After thawing, a spiked plasma sample was diluted 5x and 25x with TBS to give three concentrations of 10 ng/30 μl, 2 ng/30 μl and 0.4 ng/30 μl, respectively, representing the useful range of the calibration curve. Data pairs were calibrated using background adjustment, as described above, in triplicate on 13 different days to investigate intra-day and inter-day sources of variation. Coefficients of variation (CV) representing intra-day and inter-day variances were estimated via one-way analysis of variance employing Excel (v. 14, Microsoft Office 2010).

Statistical analyses

BPDE-HSA concentrations in plasma were normalized by the corresponding HSA content with units of ng BPDE-HSA/mg HSA. Since BPDE-HSA concentrations in both sets of validation samples covered large ranges and were right skewed, natural logarithmic transformation was applied to satisfy normality assumptions for statistical testing. Samples with measurements below the DL were imputed a value of half the DL for statistical analysis.

For the smoker/nonsmoker data, generalized linear models were used to determine the effects of smoking, gender and their interaction on BPDE-HSA levels. Because each smoker/nonsmoker sample had been pooled from 4 or 5 subjects, simple linear regression of logged BPDE-HSA levels on smoking intensity employed the average number of cigarettes smoked per day. The data from highway workers included repeated measurements from individual subjects during different seasons of the year. Thus, mixed-effects models were used with subject as a random effect and with season, job and/or task as fixed effects. Restricted maximum likelihood estimation was used, assuming compound symmetry and common within-worker and between-worker variance components for the highway-paving and highway-construction workers. Statistical analyses were performed with software from SAS (v. 9.3, SAS Corp., Cary, NC).

Results & Discussion

BPDE Modification sites on HSA

Day *et al.* [29; 41] suggested that His146, Asp187 and Glu188 were likely sites for BPDE modification of HSA but did not provide confirmatory data. Using an intact BPDE-HSA standard, we previously reported that about 80% of modified HSA contained one BPDE modification and about 20% contained 2 BPDE modifications [36], indicating that at least 2 modification sites were involved. Here we performed proteomic analysis of a tryptic digest of BPDE-HSA to pinpoint the binding sites. Figure 3 shows ETD and CID MS/MS spectra of 2 modified peptides, RHPYFYAPELLFFAK (seq. # 145–159) and ASSAKQR (seq. # 191–197). These host peptides exhibit a monoisotopic mass increase of 302.094294 Da ± 5 ppm and were miscleaved at Arg145 and Lys195, probably due to steric hindrance imposed by the BPDE modification in the vicinity of the cleavage sites.

The CID MS/MS spectrum of the triply charged ion of modified peptide RHPYFYAPELLFFAK (734.7 *m/z*) shows a poor fragmentation pattern with the one charge-reduced native peptide (doubly charged ion at 950.3 *m/z*) and three ions at 303, 285 and 257 *m/z* (Figure 3c). This CID fragmentation pattern was reported by Day *et al.* [29] as being typical of BPDE. The same behavior was observed for the doubly charged ion (525.3 *m/z*) of modified peptide ASSAKQR (Figure 3d) and confirms that both peptides were modified by BPDE. Although CID fragmentation gives no information about locations of covalent bonds formed by BPDE binding, ETD MS/MS spectra of the same precursor ions allow His146 and Lys195 to be confirmed as the modified sites. Specifically, for the peptide RHPYFYAPELLFFAK, the series of unmodified z ions and modified c ions, along with the unmodified c_1 fragment, leads to unequivocal assignment of His146 as a binding site (Figure 3a). For Lys195 the identification is not as straightforward because the low charge state of the precursor ion hinders the ETD fragmentation (no other charge state precursor ions for peptide ASSAKQR were detected). The spectrum shows the modified z ion series plus some unmodified z ions (Figure 3b), confirming that the BPDE modification of this peptide is very labile. The presence of modified c_8 and z_3 fragments confirm that the modification occurred at Gln196 or Lys195. The non-nucleophilicity of Gln plus the missed cleavage in correspondence with Lys195 strongly points to modification of Lys195. Since there was

greater than a 5-fold difference in signal intensities between the two modified peptides, we confirm His146 as the major binding site.

Although we did not detect esters formed by reactions between BPDE and carboxylic acid side chains of Asp187 and Glu188 [29], we note that such ester adducts are labile and could have been hydrolyzed under the conditions of digestion we employed or due to steric hindrance.

Revised sandwich ELISA

Despite a 5-fold reduction in the DL (from 1 ng BPDE/mg HSA to 0.2 ng BPDE/mg HSA) we encountered difficulties when measuring BPDE-HSA directly in plasma with our original ELISA design [36]. High intra-sample variability and inter-sample variability were observed in apparent BPDE-HSA levels across sets of plasma that, given their sources, could not be attributed to BaP exposure. Rather, it appeared that some unknown interfering species in the plasma were the causes. We observed that centrifugation of the plasma at 13,000 g for 10 min greatly reduced the background levels in some samples.

Since all human plasma contains HSA at about one mM, small amounts of unadducted HSA can be adsorbed by well surfaces and then detected (at nM concentrations) by the anti-HSA antibody, thereby creating a high background signal. Yet the extent of nonspecific HSA binding reflects the particular milieu of serum proteins in a plasma specimen and is thus sample specific. We also observed that the ELISA was sensitive to unknown interfering species that varied within and between sets of samples. The characteristics of interferences match descriptions of heterophilic antibodies that can bind to more than one antigen and to other species' immunoglobulins [42; 43; 44; 45]. In any case, the anti-HSA detection antibody is susceptible to cross reactivity with features that are also sample specific. And finally, the shape of the sigmoid ELISA calibration curve is correlated with the background level in a plasma specimen and is, again, sample specific.

Since the above combination of sample-specific factors effectively precludes a global background-matching scheme, we redesigned the ELISA by splitting each plasma specimen into background and sample pairs (Figure 1), blocking the activity of the 8E11 capture antibody with BPDE tetrols in the background well to provide a matched control (Figure 1), and adjusted the calibration curve for sample-specific background readings (Figure 2). To our knowledge, this is the first application of ELISA that systematically addresses such a combination of sample-specific factors.

The magnitudes of the background effects can be gauged by the first two rows of Table 1, which show absorbance measurements with and without addition of BPDE tetrols to the control wells of BPDE-HSA standards at 0.4, 2 and 10 ng. Addition of BPDE tetrols reduced the absorbance by 28% at 0.4 ng, 54% at 2 ng and 71% at 10 ng. The positive biases associated with these background effects was about 60% to 70% over the dynamic range of the assay as indicated by the recoveries of standards listed in Table 1 with and without background adjustment.

The precision of the ELISA is indicated by the CVs given in Table 1 for three sets of triplicate standards at 0.4, 2 and 10 ng BPDE-HSA per well that were assayed on 13 different days. With background adjustment, CVs varied between 5.05% and 17.2% and were comparable for both intraday and interday components of variation.

Data screening to improve accuracy

Immunoassays are prone to interferences and matrix effects when used for measuring exposure or diagnostic biomarkers in blood [46; 47]. Interferences can be either analyte-independent (e.g. due to anticoagulants and conditions of sample storage) or analyte-dependent (e.g. heterophilic, auto-antibodies and human anti-animal antibodies and rheumatoid factors) and can result in either positive or negative biases. Although diluting samples and increasing the sample number can reduce the magnitudes of biases, these workarounds become problematic when analyte concentrations are very low, as is the case for BPDE-HSA in the general population.

Although our redesigned ELISA for BPDE-HSA includes sample-specific adjustments to reduce measurement errors, background readings differed across sets of samples (e.g. were much greater for highway workers than smokers/nonsmokers) suggesting that study-specific factors such as anticoagulants, Ficoll reagents and storage conditions also affected the ELISA. Furthermore, within a set of plasma samples, data pairs were occasionally observed where the background reading (*min*) was greater than the experimental reading (*y*) and replicates of a given plasma sample occasionally differed by several fold.

To minimize the introduction of erroneous data into statistical analysis, we performed assays of all samples in quadruplicate. These 4 replicates allowed us to flag samples where either the background reading exceeded the sample reading or at least 10-fold variation was observed across replicates. Such samples were retested and, if flagged a second time, were excluded from statistical analysis (Figure 1). Results from our 115 validation samples (35 smokers/nonsmokers and 80 highway workers) flagged 32% of samples for retesting and excluded 10% from statistical analysis (Tables 2 and 3).

Validation with plasma from smokers and nonsmokers

Since smoking is an important source of BaP exposure in the general population, we used ELISA to measure BPDE-HSA in 35 samples of pooled plasma from 158 young healthy volunteer subjects [37] (18 pooled samples from males and 17 from females). After applying the screening rules, 3 plasma samples were excluded from statistical analysis (all females). Summary statistics are shown in Table 2 for adduct levels stratified by sex and smoking status. (Preliminary analysis showed no effect of race on BPDE-HSA levels). A model containing effects for smoking, sex and their interaction was marginally significant ($P = 0.071$, $R^2 = 0.218$, $n = 32$) and showed a significant effect of the sex*smoking interaction ($P = 0.028$). Subset analysis showed that smoking had a significant effect on logged adduct levels among males ($P = 0.035$, $R^2 = 0.249$, $n = 18$) but not females ($P = 0.342$, $R^2 = 0.075$, $n = 14$). Simple linear regressions of logged BPDE-HSA levels upon the number of cigarettes smoked per day indicated that smoking intensity was a significant predictor of

logged adduct levels for males ($P = 0.016$, $R^2 = 0.310$, $n = 18$) but not for females ($P = 0.782$, $R^2 = 0.007$, $n = 14$).

Our ELISA results provide evidence that cigarette smoking increases levels of BPDE-HSA in pooled plasma from male subjects. Although we don't know why a similar effect was not observed in female subjects, it is possible that female plasma contains more interfering species than male plasma. In fact, our screening rule excluded only 3 of the 35 pooled plasma samples from smokers/nonsmokers, all of which were from female subjects (one from nonsmokers and two from smokers). The lack of association between smoking and BPDE-HSA levels among females could also reflect the small sample size in our study ($n = 17$). Two previous studies used competitive ELISA with purified HSA to detect marginal-to-significant differences in levels of BPDE tetrols between smoking and nonsmoking mothers with 75 ($P < 0.05$) and 128 ($P = 0.108$) subjects, respectively [48; 49].

Validation with plasma from highway workers

We analyzed 80 archived plasma samples from a previous study of highway workers that had investigated lymphocytic DNA adducts [39] and urinary 1-hydroxypyrene [38] as potential biomarkers of asphalt exposure. All of the workers in the current sample were nonsmokers. Results of these analyses are shown in Table 3. Since the 80 plasma specimens had been collected from 37 workers (28 paving and 9 construction workers) during either 2 or 3 seasons of the year, mixed effect models were used to estimate effects of job, task and season of the year on logged BPDE-HSA levels. When all valid samples were included in the model ($n = 68$), no difference was observed in geometric mean (GM) adduct concentrations between the paving workers exposed to hot asphalt (GM = 1.55 ng BPDE-HSA/mg HSA) and the highway construction workers who were not exposed to asphalt emissions (GM = 1.53 ng BPDE-HSA/mg HSA). When valid samples were investigated across seasons of the year, however, BPDE-HSA levels were found to be 2-fold higher in the winter (GM = 2.39 ng BPDE-HSA/mg HSA) than in the other seasons (GM = 1.15–1.37 ng BPDE-HSA/mg HSA) ($P < 0.001$). Interestingly, in the original study DNA-adduct levels were also found to be significantly higher during the winter season [39]. Since these highway workers did not work during the winter, this suggests that the major BaP exposures experienced by this population arose from non-occupational sources that were more pronounced during the winter. To investigate the contributions of occupational factors *per se*, we excluded samples collected during the winter and tested for differences in adduct levels across the job tasks ($n = 58$). As shown in Table 3, the estimated GM concentration of BPDE-HSA (ng/mg HSA) increased in the following order: construction worker (1.18) < paver operator (1.20) < raker (1.29) < screedman (1.55), a difference of 30% that was marginally significant ($P = 0.070$). Interestingly, screedmen had also been identified as the most heavily PAH-exposed subjects in the original study, based upon both BPDE-DNA [39] and urinary 1-hydroxypyrene [38]. Thus, ELISA measurements of BPDE-HSA in this subset of plasma samples recapitulated results from the more extensive sets of measurements originally reported.

In summary, our redesigned ELISA can measure BPDE-HSA at very low concentrations (at or above 0.2 ng/mg HSA, equivalent to 3.28 fmol BPDE equivalents/mg HSA) in human

plasma without sample pretreatment and without conversion of adducts to BPDE tetrols. We confirmed that BPDE forms stable *N*-substituted adducts with HSA primarily at His146 and to a lesser extent with Lys195. By performing analyses in quadruplicate, with and without addition of BPDE tetrols to deactivate the capture antibody (8E11), we incorporated a series of sample-specific adjustments and screening steps to reduce measurement errors that are a consequence of assaying low BPDE-HSA levels in the general population. Applications of the ELISA to sets of plasma - from smoking/nonsmoking subjects and highway workers from jobs with and without use of asphalt - detected differences in BPDE-HSA in the *a priori*-expected directions. The ELISA should be suitable for investigating sources and effects of PAH exposure in the general population.

Acknowledgments

Financial support for this work was provided by a contract from the Long-range Research Initiative of the American Chemistry Council and by grant U54ES016115 from the U.S. National Institute of Environments Health Sciences (NIEHS) through the trans-NIH Genes, Environment, and Health Initiative. The authors are grateful to Anthony Iavarone for assistance with mass spectrometry.

Abbreviations Used:

ABC	avidin-biotin complex
BaP	benzo[*a*]pyrene
BPDE	benzo[*a*]pyrene diolepoxide
BPDE-HSA	adducts of BPDE with human serum albumin
BPDE tetrols	benzo[*a*]pyrene-r-7, t-8, t-9, c-10-tetrahydrotetrol(+/−)
CID	collision induced dissociation
CV	coefficient of variation
DL	detection limit
DMSO	dimethylsulfoxide
ELISA	enzyme-linked immunosorbent assays
ESI	electro-spray ionization
ETD	electron transfer dissociation
HSA	human serum albumin
HRP	horseradish peroxidase
HPLC	high-performance liquid chromatography
MS	mass spectrometry
NFDM	nonfat dry milk

PAHs	polycyclic aromatic hydrocarbons
PBS	phosphate-buffered saline
TBS	tris-buffered saline
TCEP	tris(2-carboxyethyl)phosphine
TMB	3,3',5,5'-tetramethylbenzidine

References

[1]. Khalili NR, Scheff PA, and Holsen TM, PAH source fingerprints for coke ovens, diesel and, gasoline engines, highway tunnels, and wood combustion emissions. Atmospheric Environment 29 (1995) 533–542.

[2]. Xu S, Liu W, and Tao S, Emission of Polycyclic Aromatic Hydrocarbons in China. Environmental Science & Technology 40 (2006) 702–708. [PubMed: 16509306]

[3]. Boffetta P, Jourenkova N, and Gustavsson P, Cancer risk from occupational and environmental exposure to polycyclic aromatic hydrocarbons. Cancer Causes and Control 8 (1997) 444–72. [PubMed: 9498904]

[4]. Bosetti C, Boffetta P, and La Vecchia C, Occupational exposures to polycyclic aromatic hydrocarbons, and respiratory and urinary tract cancers: a quantitative review to 2005. Annals of Oncology 18 (2007) 431–46. [PubMed: 16936186]

[5]. Straif K, Baan R, Grosse Y, Secretan B, El Ghissassi F, and Cogliano V, Carcinogenicity of polycyclic aromatic hydrocarbons. The Lancet Oncology 6 (2005) 931–932. [PubMed: 16353404]

[6]. Choi H, Jedrychowski W, Spengler J, Camann DE, Whyatt RM, Rauh V, Tsai W-Y, and Perera FP, International studies of prenatal exposure to polycyclic aromatic hydrocarbons and fetal growth. Environmental health perspectives 114 (2006) 1744–1750. [PubMed: 17107862]

[7]. Perera FP, Rauh V, Tsai W-Y, Kinney P, Camann D, Barr D, Bernert T, Garfinkel R, Tu Y-H, Diaz D, Dietrich J, and Whyatt RM, Effects of transplacental exposure to environmental pollutants on birth outcomes in a multiethnic population. Environmental Health Perspectives 111 (2003) 201–205. [PubMed: 12573906]

[8]. Perera FP, Tang D, Wang S, Vishnevetsky J, Zhang B, Diaz D, Camann D, and Rauh V, Prenatal polycyclic aromatic hydrocarbon (PAH) exposure and child behavior at age 6–7 years. Environmental health perspectives 120 (2012) 921–926. [PubMed: 22440811]

[9]. Perera FP, Wang S, Vishnevetsky J, Zhang B, Cole KJ, Tang D, Rauh V, and Phillips DH, Polycyclic aromatic hydrocarbons-aromatic DNA adducts in cord blood and behavior scores in New York city children. Environmental health perspectives 119 (2011) 1176–1181. [PubMed: 21486719]

[10]. Chung MK, Hu R, Cheung KC, and Wong MH, Pollutants in Hong Kong soils: Polycyclic aromatic hydrocarbons. Chemosphere 67 (2007) 464–473. [PubMed: 17109918]

[11]. Lodovici M, Venturini M, Marini E, Grechi D, and Dolara P, Polycyclic aromatic hydrocarbons air levels in Florence, Italy, and their correlation with other air pollutants. Chemosphere 50 (2003) 377–382. [PubMed: 12656258]

[12]. Whitehead T, Metayer C, Gunier RB, Ward MH, Nishioka MG, Buffler P, and Rappaport SM, Determinants of polycyclic aromatic hydrocarbon levels in house dust. Journal of exposure science & environmental epidemiology 21 (2011) 123–132. [PubMed: 20040932]

[13]. Zhou JL, and Maskaoui K, Distribution of polycyclic aromatic hydrocarbons in water and surface sediments from Daya Bay, China. Environmental Pollution 121 (2003) 269–281. [PubMed: 12521113]

[14]. Kavouras IG, Koutrakis P, Tsapakis M, Lagoudaki E, Stephanou EG, Von Baer D, and Oyola P, Source Apportionment of Urban Particulate Aliphatic and Polynuclear Aromatic Hydrocarbons

(PAHs) Using Multivariate Methods. Environmental Science & Technology 35 (2001) 2288–2294. [PubMed: 11414034]

[15]. Gelboin HV, Benzo[alpha]pyrene metabolism, activation and carcinogenesis: role and regulation of mixed-function oxidases and related enzymes. Physiological reviews 60 (1980) 1107–1166. [PubMed: 7001511]

[16]. Liebler DC, Protein Damage by Reactive Electrophiles: Targets and Consequences. Chemical Research in Toxicology 21 (2008) 117–128. [PubMed: 18052106]

[17]. Poirier MC, and Weston A, Human DNA adduct measurements: state of the art. Environmental health perspectives 104 Suppl 5 (1996) 883–893. [PubMed: 8933030]

[18]. Phillips DH, and Arlt VM, The 32P-postlabeling assay for DNA adducts. Nature protocols 2 (2007) 2772–2781. [PubMed: 18007613]

[19]. Godschalk RW, Van Schooten FJ, and Bartsch H, A critical evaluation of DNA adducts as biological markers for human exposure to polycyclic aromatic compounds. Journal of Biochemistry and Molecular Biology 36 (2003) 1–11. [PubMed: 12542969]

[20]. Knudsen LE, Ryder LP, and Wassennann K, Induction of DNA Repair Synthesis in Human Monocytes/B-Lymphocytes Compared with T-Lymphocytes After Exposure to N-Acetoxy-N-Acetylaminofluorene and Dimethylsulfate in Vitro. Carcinogenesis 13 (1992) 1285–1287. [PubMed: 1638700]

[21]. Beach AC, and Gupta RC, Human biomonitoring and the 32P-postlabeling assay. Carcinogenesis 13 (1992) 1053–1074. [PubMed: 1638670]

[22]. Phillips DH, Hewer A, and Arlt VM, 32P-Postlabeling Analysis of DNA Adducts, Molecular Toxicology Protocols, 2004, pp. 3–12.

[23]. Phillips DH, and Castegnaro M, Results of an interlaboratory trial of 32P-postlabelling. IARC scientific publications (1993) 35–49. [PubMed: 8225506]

[24]. Phillips DH, and Castegnaro M, Standardization and Validation of DNA Adduct Postlabelling Methods: Report of Interlaboratory Trials and Production of Recommended Protocols. Mutagenesis 14 (1999) 301–315. [PubMed: 10374998]

[25]. Brown K, Methods for the Detection of DNA Adducts. in: Parry JM, Parry EM, and Walker JM, (Eds.), Genetic Toxicology, Springer New York, 2012, pp. 207–230.

[26]. Hollstein M, Sidransky D, Vogelstein B, and Harris CC, p53 mutations in human cancers. Science (New York, N.Y.) 253 (1991) 49–53.

[27]. Braithwaite E, Wu X, and Wang Z, Repair of DNA lesions: mechanisms and relative repair efficiencies. Mutation research 424 (1999) 207–219. [PubMed: 10064862]

[28]. Day BW, Doxtader MM, Rich RH, Skipper PL, Singh K, Dasari RR, and Tannenbaum SR, Human serum albumin-benzo[a]pyrene anti-diol epoxide adduct structure elucidation by fluorescence line narrowing spectroscopy. Chem. Res. Toxicol 5 (1992) 71–76. [PubMed: 1581540]

[29]. Day BW, Skipper PL, Zaia J, and Tannenbaum SR, Benzo[a]pyrene anti-diol epoxide covalently modifies human serum albumin carboxylate side chains and imidazole side chain of histidine(146). J. Am. Chem. Soc 113 (1991) 8505–8509.

[30]. Lee BM, Yin BY, Herbert R, Hemminki K, Perera FP, and Santella RM, Immunologic measurement of polycyclic aromatic hydrocarbon-albumin adducts in foundry workers and roofers. Scand J Work Environ Health 17 (1991) 190–4. [PubMed: 2068558]

[31]. Sherson D, Sabro P, Sigsgaard T, Johansen F, and Autrup H, Biological monitoring of foundry workers exposed to polycyclic aromatic hydrocarbons. Br J Ind Med 47 (1990) 448–53. [PubMed: 2383513]

[32]. Käfferlein HU, Marczynski B, Mensing T, and Brüning T, Albumin and hemoglobin adducts of benzo[a]pyrene in humans--analytical methods, exposure assessment, and recommendations for future directions. Critical reviews in toxicology 40 (2010) 126–150. [PubMed: 20085480]

[33]. Lee BM, and Santella RM, Quantitation of protein adducts as a marker of genotoxic exposure: immunologic detection of benzo[a]pyrene--globin adducts in mice. Carcinogenesis 9 (1988) 1773–7. [PubMed: 3168157]

[34]. Tas S, Buchet JP, and Lauwerys R, Determinants of benzo[a]pyrene diol epoxide adducts to albumin in workers exposed to polycyclic aromatic hydrocarbons. International archives of occupational and environmental health 66 (1994) 343–348. [PubMed: 7896420]

[35]. Verma N, Pink M, Rettenmeier AW, and Schmitz-Spanke S, Review on proteomic analyses of benzo(a)pyrene toxicity. PROTEOMICS (2012).

[36]. Chung MK, Riby J, Li H, Iavarone AT, Williams ER, Zheng Y, and Rappaport SM, A sandwich enzyme-linked immunosorbent assay for adducts of polycyclic aromatic hydrocarbons with human serum albumin. Analytical Biochemistry (2010).

[37]. Lin YS, McKelvey W, Waidyanatha S, and Rappaport SM, Variability of albumin adducts of 1,4-benzoquinone, a toxic metabolite of benzene, in human volunteers. Biomarkers 11 (2006) 14–27. [PubMed: 16484134]

[38]. McClean MD, Rinehart RD, Ngo L, Eisen EA, Kelsey KT, Wiencke JK, and Herrick RF, Urinary 1-hydroxypyrene and polycyclic aromatic hydrocarbon exposure among asphalt paving workers. Annals of Occupational Hygiene 48 (2004) 565–578. [PubMed: 15292037]

[39]. McClean MD, Wiencke JK, Kelsey KT, Varkonyi A, Ngo L, Eisen EA, and Herrick RF, DNA adducts among asphalt paving workers. Annals of Occupational Hygiene 51 (2007) 27–34. [PubMed: 17046959]

[40]. Keller BO, Sui J, Young AB, and Whittal RM, Interferences and contaminants encountered in modern mass spectrometry. Anal Chim Acta 627 (2008) 71–81. [PubMed: 18790129]

[41]. Day BW, Skipper PL, Zaia J, Singh K, and Tannenbaum SR, Enantiospecificity of Covalent Adduct Formation by Benzo[a]pyrene anti-Diol Epoxide with Human Serum Albumin. Chem. Res. Toxicol 7 (1994) 829–835. [PubMed: 7696539]

[42]. Bjerner J, Børmer OP, and Nustad K, The War on Heterophilic Antibody Interference. Clinical Chemistry 51 (2005) 9–11. [PubMed: 15613705]

[43]. Fahie-Wilson M, and Halsall D, Polyethylene glycol precipitation: proceed with care. Annals of Clinical Biochemistry 45 (2008) 233–235. [PubMed: 18482908]

[44]. Ismail AAA, A Radical Approach Is Needed to Eliminate Interference from Endogenous Antibodies in Immunoassays. Clinical Chemistry 51 (2005) 25–26. [PubMed: 15539464]

[45]. Ismail AAA, Interference from endogenous antibodies in automated immunoassays: what laboratorians need to know. Journal of clinical pathology 62 (2009) 673–678. [PubMed: 19638536]

[46]. Chiu NHL, and Christopoulos TK, Advances in Immunoassay Technology, InTech, Rijeka, Croatia, 2012.

[47]. Hoofnagle AN, and Wener MH, The fundamental flaws of immunoassays and potential solutions using tandem mass spectrometry. Journal of immunological methods 347 (2009) 3–11. [PubMed: 19538965]

[48]. Crawford FG, Mayer J, Santella RM, Cooper TB, Ottman R, Tsai WY, Simon-Cereijido G, Wang M, Tang D, and Perera FP, Biomarkers of environmental tobacco smoke in preschool children and their mothers. Journal of the National Cancer Institute 86 (1994) 1398–1402. [PubMed: 8072033]

[49]. Autrup H, Vestergaard AB, and Okkels H, Transplacental transfer of environmental genotoxins: polycyclic aromatic hydrocarbon-albumin in non-smoking women, and the effect of maternal GSTM1 genotype. Carcinogenesis 16 (1995) 1305–1309. [PubMed: 7788847]

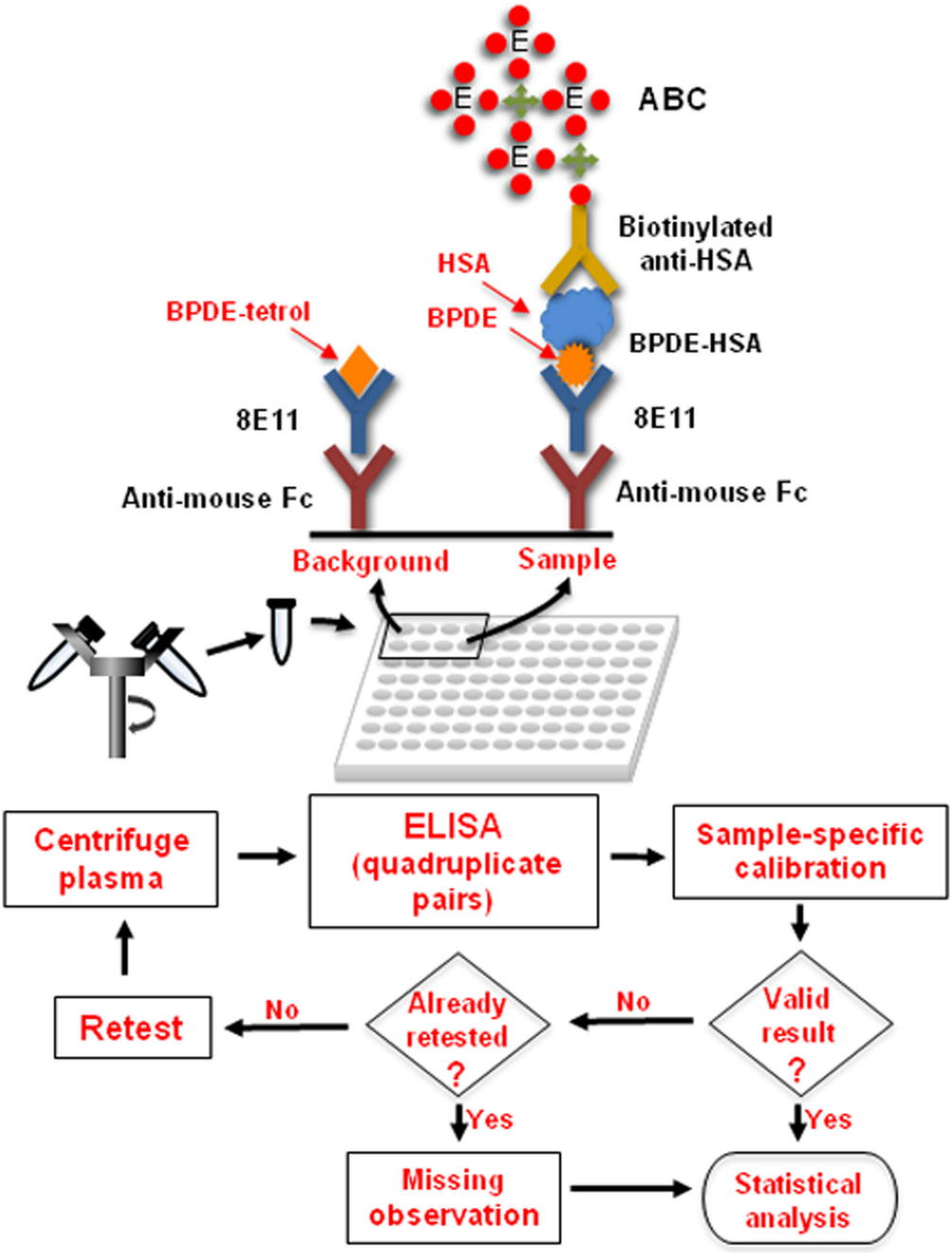

Figure 1.

Sandwich ELISA for direct measurement of BPDE-HSA in plasma. After centrifugation, plasma is mixed with reagents and loaded into pairs of wells in a pre-coated plate. Because the anti-HSA detection antibody responds to both BPDE-HSA (about one nM in plasma) and unadducted HSA (about one mM in plasma), a high background signal is created from amplification of non-specifically bound HSA on well surfaces. To overcome this problem, paired measurements (‘background’ and ‘sample’) are obtained for each plasma sample in quadruplicate and the signals are deconvoluted and calibrated by a sample-specific

calibration method (Figure 2). Background wells are treated with BPDE tetrols to deactivate the capture antibody (8E11) and thereby to produce matched controls. To minimize measurement errors, each result is screened for validity using predetermined rules. Valid samples are used for statistical analyses and invalid samples are treated as missing observations.

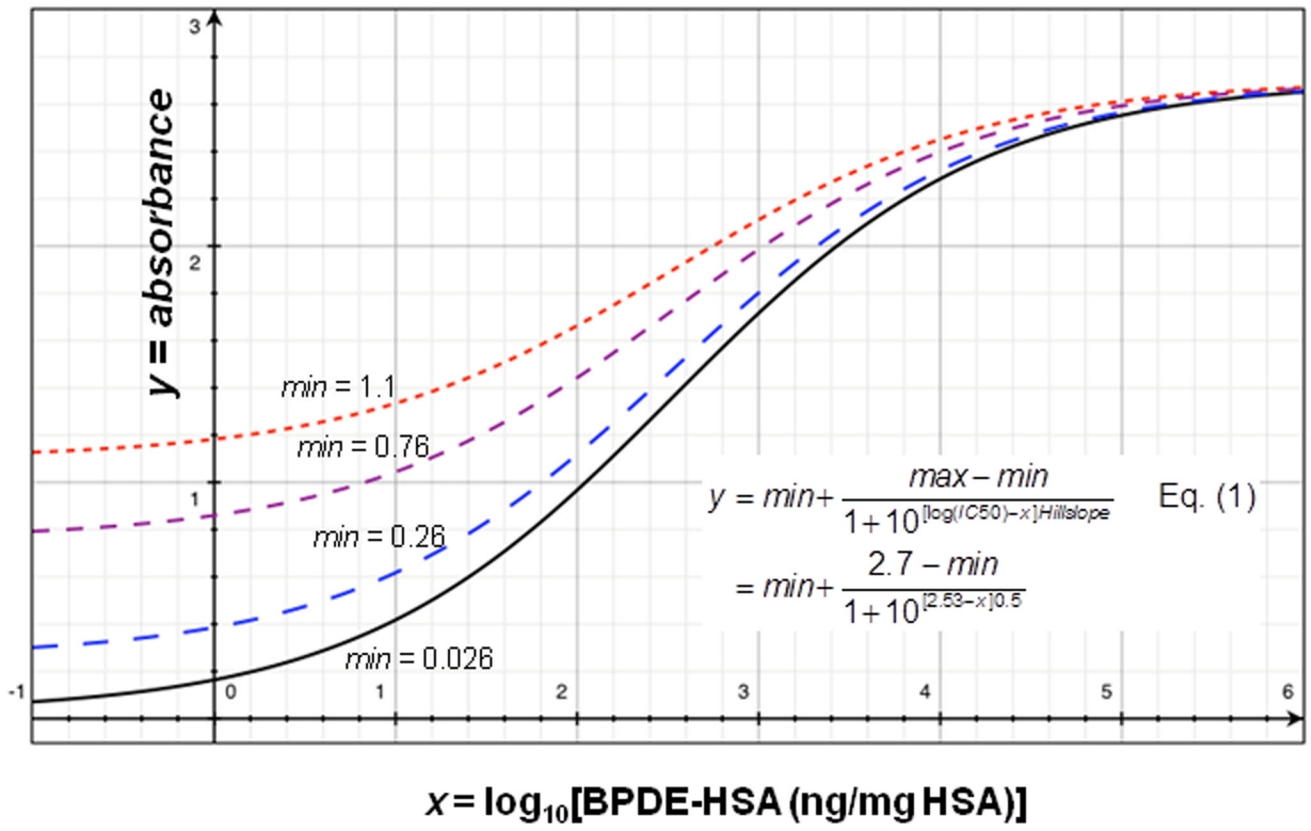

Figure 2.

Sample-specific calibration curves for quantitation of BPDE-HSA by ELISA. Each standard or plasma sample is split into pairs of wells to determine 'background' (*min*) and 'sample' (*y*) absorbance readings (see Figure 1). A set of BPDE-HSA standards is used to develop a sigmoid standard curve [Eq. (1)], the shape of which is influenced by the particular background reading (*min*). The solid curve represents a standard curve obtained from BPDE-HSA standards (in buffer) where *min* = 0.026 absorbance units, *max* = 2.7 absorbance units, log(*IC50*) = 2.53 and *Hillslope* = 0.5. Having established the standard curve with buffer solutions, the value of *min* for each plasma specimen is substituted into Eq. (1) to solve for 10^x, representing the concentration of BPDE-HSA (ng/mg HSA) in that plasma specimen. The three dashed curves in the figure represent background plasma readings where *min* = 0.26, 0.76 and 1.1 absorbance units, respectively.

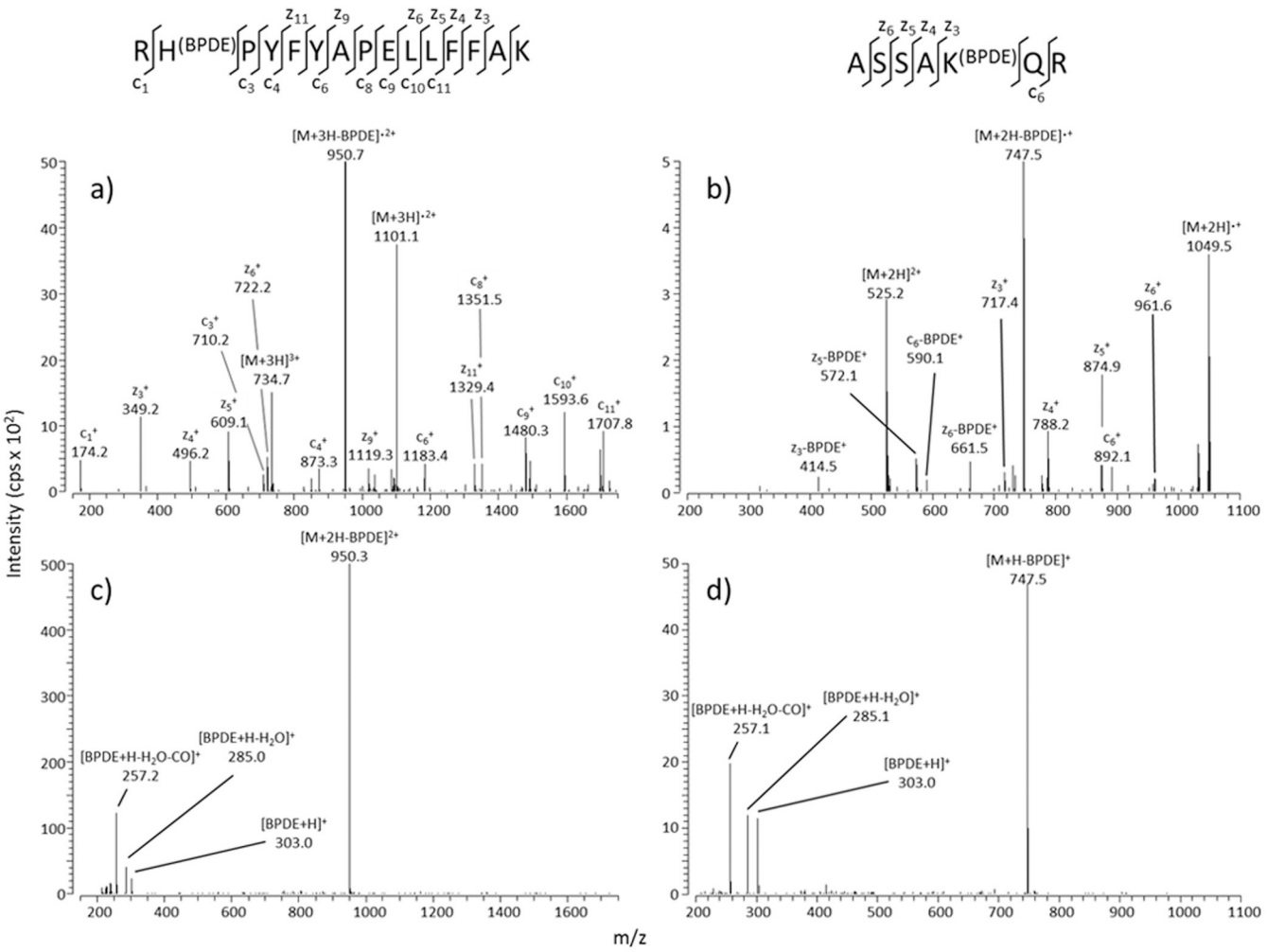

Figure 3.

Tandem mass spectra of the triply charged precursor ion at *m/z* 734.70 (BPDE adduct of peptide RHPYFYAPELLFFAK) obtained by ETD activation (a) or CID activation (c) and tandem mass spectra of the doubly charged precursor ion at *m/z* 525.25 (BPDE adduct of peptide ASSAKQR) obtained by ETD activation (b) or CID activation (d).

Table 1.

Accuracy and precision of the ELISA with different amounts of BPDE-HSA. (Three sets of triplicate experimental/background pairs of spiked plasma were analyzed on 13 different days).

	BPDE-HSA added					
	0.4 ng		**2 ng**		**10 ng**	
BPDE tetrols added?	Yes	No	Yes	No	Yes	No
Absorbance	0.175	0.222	0.341	0.583	0.786	1.679
Recovery (%)						
Background adjusted	103		104		115	
Not background adjusted	164		176		177	
CV (%)	Intraday	Interday	Intraday	Interday	Intraday	Interday
	17.2	7.50	5.05	6.37	7.55	14.4

Table 2.

ELISA measurements of BPDE-HSA in smokers and nonsmokers (archived specimens from [37]).

Characteristic	No. Samples[b]	No. excluded	BPDE-HSA (ng/mg HSA)[a] Geo. mean	Min.	Max.
Male					
Nonsmokers	8	0	0.529	0.280	1.08
Smokers	10	0	0.941	0.356	2.88
Total	*18*	*0*	*Fold change = 1.78*[c]		
Female					
Nonsmokers	7	1	0.710	0.412	1.20
Smokers	10	2	0.577	0.335	1.25
Total	*17*	*3*	*Fold change = 0.813*		

[a] Note that 1 ng/mg HSA is equivalent to 16.4 fmol BPDE equivalents/mg HSA.

[b] Each sample represents plasma pooled from 4 or 5 subjects.

[c] *P*-value = 0.016.

Table 3.

ELISA measurements of BPDE-HSA in highway workers (archived specimens from [38; 39]).

Characteristic	No. subjects	No. samples	No. excluded	BPDE-HSA (ng/mg HSA)[a] Geo. mean	Min.	Max.
Job						
Paving	28	56	4	1.55	0.475	13.9
Construction	9	24	8	1.53	0.346	6.08
Total	*37*	*80*	*12*	*Fold change= 1.01*		
Season						
Spring		8	0	1.15	0.620	2.15
Summer		31	5	1.37	0.475	5.99
Fall		15	7	1.29	0.346	4.56
Winter		26	0	2.39	0.556	13.9
Total	*37*	*80*	*12*	*Fold change = 2.08*[b]		
Task						
Construction	9	16	4	1.18	0.346	5.99
Paver operator	4	6	1	1.20	0.475	2.15
Raker	15	21	0	1.29	0.525	4.56
Screedman	9	11	0	1.55	0.538	3.36
Total	*37*	*54*	*5*	*Fold change = 1.31*[c]		

[a] Note that 1 ng/mg HSA is equivalent to 16.4 fmol BPDE equivalents/mg HSA.

[b] *P*-value < 0.001.

[c] *P*-value = 0.070.